Study of thermal comfort and air diffusion induced by a heated airflow window

Alain Makhour, Ghislain Michaux, Patrick Salagnac, Pierre Bragança

Journal of Building Engineering 129 (2026) 116789

Contents lists available at ScienceDirect

Journal of Building Engineering

journal homepage: www.elsevier.com/locate/jobe

Study of thermal comfort and air diffusion induced by a heated airflow window

Alain Makhour [a], Ghislain Michaux [b,*], Patrick Salagnac [b], Pierre Bragança [c]

[a] BDR Thermea France, De Dietrich Thermique, 57 Rue de la Gare, Mertzwiller, 67580, France
[b] LaSIE, UMR-CNRS 7356, La Rochelle Université, Av. M. Crépeau, Cedex 1, La Rochelle, 17042, France
[c] LMFL, UMR-CNRS 9014, Université de Lille, Av. P. Langevin, Villeneuve d'Ascq, Cedex, 59655, France

ARTICLE INFO

Keywords:
Building
Heated airflow window
Experimentation
Thermal comfort
Indoor air quality

ABSTRACT

Windows are a critical component in the thermal performance of building envelopes. For cold climates, airflow windows have been developed in order to simultaneously reduce thermal losses in winter through windows and caused by ventilation systems. However, such windows can induce a risk of "cold wall" effect, due to a lower inner window surface temperature, which can negatively impact the thermal comfort of occupants. For this reason, an airflow window has been improved by incorporating an electric heating film into its inner glass pane. Thus, the resulting heated airflow window also acts as a radiating panel for building space heating applications. However, in that case and unlike conventional heated glazing, direct thermal loss to outdoor are reduced, being partly recovered by the fresh air coming from the outside and flowing between the window glass panes before its introduction into the building.

This paper reports experimental results from a study conducted on the effect of such a heated airflow window on both thermal comfort and indoor air quality through fresh air diffusion. Two heated airflow window configurations were investigated, with upward and downward fresh air inlet, respectively. From temperature and velocity measurements performed in a climatic cell representative of a housing room, the Predicted Mean Vote (PMV) and Predicted Percent Dissatisfied (PPD) were assessed. Results pointed out that the air discharge direction had no effect on the thermal comfort as well as on local comfort parameters that were also assessed (indoor thermal stratification, radiation asymmetry and fresh air diffusion in the occupied zone).

The results were then compared to those obtained for two other configurations, namely an unheated airflow window combined with an electric convector, and a reference configuration defined as the combination of a conventional double-glazed window with the same electric convector. This comparative study was conducted by considering the same heating power, *i.e.* the same electricity consumption of both the heating film and the convector. The obtained results showed that the heated airflow window improved the thermal comfort, despite the heat losses due to the direct thermal transmission through the glazing to the outside environment. Indeed, 90% of the occupied zone was in the PMV category A, compared to only 61% when a conventional double-glazed window was used. This is mainly due to a higher window surface temperature and a better mixing of air within the occupied zone. The use of a heated airflow window also reduced thermal stratification and did not present any risk of radiation asymmetry. Moreover, the results showed that the use of a heated airflow window led to better fresh air diffusion within the occupied zone due to a better mixing of air, and thus a better indoor air quality.

* Corresponding author.
E-mail address: ghislain.michaux@univ-lr.fr (G. Michaux).

https://doi.org/10.1016/j.jobe.2026.116789
Received 23 April 2026; Received in revised form 16 June 2026; Accepted 3 July 2026
Available online 4 July 2026

Nomenclature

ACH	Air change per hour	PD	Percentage dissatisfied, %
D	Diameter, m	PMV	Predicted mean vote
F	View factor	PPD	Predicted percentage of dissatisfied, %
G	Glass	q	Heat flux density, $W.m^{-2}$
IAQ	Indoor Air Quality	Q	Flow rate, $m^3.h^{-1}$
L	Air layer	RH	Relative humidity, %
LE	Low emissivity	T	Temperature, °C or K
M	Metabolic rate, $W.m^{-2}$	v	Velocity, $m.s^{-1}$
Greek symbols			
ε	Thermal emissivity	ΔP	Pressure gap, Pa
Index and exponent			
a	ankles	ra	radiation asymmetry
g	globe	rm	radiant mean
h	head	vtg	vertical temperature gradient
out	outdoor	w	wall
pr	occupant radiant		

1. Introduction

From a thermal point of view, windows are a critical component of buildings' envelope. Studies have shown that, in winter and for cold climates, the proportion of heat loss due to windows and ventilation is around 30-40% in an existing building for alpine climates [1]. In recent and more efficient buildings, such as passive houses, Feist and Schnieders [2] showed that heat losses through windows and ventilation systems can reach 80% of the total loss (61% and 19% respectively) for central European climates in winter. Within this context, multifunctional smart windows emerged, based on various technologies, since the middle of the last century and their adoption has accelerated over the past five years [3]. Among them, airflow windows have emerged and have been developed for both heating and cooling applications for cold and hot climates respectively. However, Wei et al. [4] pointed out that the use of an airflow windows is more relevant for colder climates. In this case, thermal losses through windows and ventilation systems can simultaneously be reduced. Indeed, the airflow window considered here, composed of 3 glass panes with a single airflow [5], pre-heats the fresh air entering the building in temperate and cold climates, in addition to obviously providing access to natural light. This incoming air, necessary for air renewal, flows between the window panes and is thus preheated by partially recovering heat loss through the window as well as heat coming from solar radiation and absorbed by the glazing. Studies conducted on the energy performance of such windows revealed a 40% reduction in heat loss through glazing and ventilation, and that the heating demand of a house equipped with airflow windows can be reduced by 20-30% compared to the same house equipped with conventional double-glazed windows [5,6]. However, the fresh air flowing within the glazing of the airflow window causes a cooling effect on the inner glass pane. Therefore, in comparison to conventional double or triple glazing, this leads to a lower inner window surface temperature and, in terms of the comfort of the occupants, to a higher risk of a "cold wall" effect.

In the nineties, glazing equipped with electric heating films appeared in North America in order to provide thermal protection for the large glass facades of shopping centers and industrial buildings in cold climates. With the development of more efficient glazing, heated glazing was subsequently more widely used to reduce the risk of local discomfort for users (the "cold wall" effect) and condensation on glass panes [7–14]. However, in comparison to conventional heating systems, the main disadvantage of heated glazing comes from direct contact with the outside: part of the heat emitted is directly transmitted to the outside environment.

This paper investigates the relevance of the combination of the two aforementioned systems, namely the airflow window and the heated glazing. The main objective was to reduce this direct thermal loss of the heated glazing to outdoor, thus partly recovered by the fresh air coming from the outside and flowing between the window glass panes before its introduction into the building. This new window type, an airflow window equipped with a heated glazing, should provide the opportunity to partly recover at the same time thermal losses through the window and the ventilation system, as well as the heated glazing ones. At the same time, the window heating prevents the aforementioned "cold wall" effect observed for airflow windows.

For the present study, the airflow window previously developed and composed of 3 glass panes with a single airflow [5] has been improved by incorporating a heating film into the inner glass pane, thus acting as a radiating panel for building space heating applications in cold climates. Expected benefits were to reduce the risk of thermal discomfort as well as of condensation that may form on the internal glazing surface [15]. Moreover, since the heat emitter is thus incorporated into the building envelope, this leads to a gain in living space. Preliminary studies have been conducted by the authors on the effect of the airflow rate and the heating power on the temperature field measured by infrared thermography on the inner face of the heated airflow glazing [16], and on the performance of the heated airflow window in terms of heating energy consumption in comparison to a conventional double-glazed window [17].

The main objective of the present study was to investigate the potential of the developed heated airflow window to improve the occupants' thermal comfort as well as the indoor air quality (IAQ) due to the fresh air diffusion from the window. This study was conducted from experiments carried out in a laboratory climatic cell representing a typical housing room.

The first part of this paper describes the experimental facilities and instrumentation, as well as the two investigated heated airflow window configurations, with upward and downward fresh air inlet, respectively. Then, the experimental methodology adopted to conduct the proposed comparative study to two additional configurations is described, namely an unheated airflow window combined with an electric convector, and a reference configuration defined as the combination of a conventional double-glazed window with the same electric convector. This comparative study was conducted by considering the same heating power, *i.e.* the same electricity consumption of both the heating film and the convector.

Results from this comparative study are presented and discussed in the last part of the paper. From temperature and velocity measurements performed in the climatic cell, the Predicted Mean Vote (PMV) and Predicted Percent Dissatisfied (PPD) were assessed for all the configurations, as well as additional local comfort parameters related to the indoor thermal stratification, the radiation asymmetry and the fresh air diffusion in the occupied zone. Finally, a comparison between all the configurations is also presented and discussed in terms of IAQ.

2. Experimental setup

The experimental set-up consisted of a climatic cell equipped with thermo-regulated walls, floor and roof, a heated airflow window and an air conditioning system (Fig. 1).

2.1. Description of the climatic cell

The climatic cell, named “AIRDIFF”, is a cubic cavity representing a full-scale small room in a building. It measures 3.65 m on the outer side and 3.47 m on the inner side. Its walls, floor and roof are 90 mm thick and are thermo-regulated and insulated (thermal resistance of 3.7 $m^2 K W^{-1}$). They consist of “sandwich” panels composed of two 1 mm thick aluminum sheets, an 88 mm thick polyurethane foam insulation, and a layer of polypropylene capillary tubes (KaRo system). These capillary tubes, in which temperature-controlled water circulates, have an external diameter of 3 mm. They are connected to a 12 kW reversible heat pump (Aqualis 2 - 50 HT, CIAT). The role of the capillary tubes is to maintain the inner face of all the walls, the floor and the roof at a desired temperature, regardless of the outdoor conditions.

In order to incorporate the window under test within the climatic cell, a wooden partition was mounted as shown in Fig. 1. The window was placed in the wall and divides the climatic cell into two parts: one part represents the external environment (left on Fig. 1) and the other the internal ambience of a living space (right on Fig. 1). As described in Section 2.4.2, three windows were tested, namely a heated airflow window, an unheated airflow window and a conventional double-glazed window. For these two last windows, the investigated configurations consisted of combining the window with an electric convector for heating as shown by Fig. 1and Fig. 7.

The objective was to study the behavior of these various windows for cold climates, without solar gain and under steady state laboratory conditions. Therefore, on the back of the window, a box connected to an aeraulic circuit and a cooling unit was set up to adjust in real time the temperature of the simulated outdoor air which then entered the climatic cell through the window. The cooling unit consists of a fan coil unit and a heat exchanger linked to a chiller. The fan coil unit generates the required airflow. The fan coil heat exchanger (CIAT), which cools the air before it enters the climatic cell through the window, is connected to a chiller (Huber Unichiller 050-H). The cooling capacity at 0°C is 4.2 kW and the temperature stability at −10°C is ±0.2°C.

The fan coil unit supplies a cold airflow to the box which covers the entire outer face of the window. Thus, this box simulates outdoor cold climate conditions. Part of the airflow ($Q = 15\ m^3/h$) enters the climatic cell through the window while the rest is returned to the fan coil unit, as shown in Fig. 1. The homogeneity of the temperature at the outer face of the window, as well as that of the air inside the box, was checked by making preliminary temperature measurements using K type thermocouples (see next section) and an infrared camera.

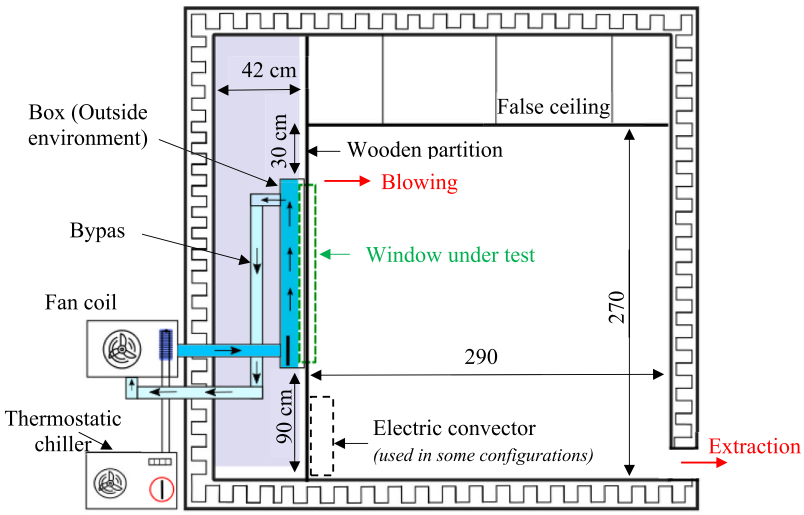

Fig. 1. Experimental device: climatic cell characteristics and location of the window under test (associated to an electric convector in some investigated configurations).

2.2. Geometrical and physical characteristics of the heated airflow window

The heated airflow window is illustrated by Figs. 2 and 3. It consists of three glass panes and two air layers through which the fresh air circulates before it enters the climatic cell. By convention, as shown in Fig. 3, the glass pane faces are numbered from the outside in. Therefore, face 1 corresponds to the outer face of the glazing, while face 6 corresponds to its inner face, in contact with the indoor air.

The air layers L_1 (outer side) and L_2 (inner side) are 22 and 20 mm thick, respectively. The outer glass panes G_1 and G_2 are 4 mm thick. The inner glass pane G_3 is a laminated glass consisting of two 3.5 mm thick glass panes. As shown by Fig. 3, the heating film was encapsulated between these two glass panes of the glass pane G_3. The enclosed heating film was similar to the layers used for low-emissivity treatments obtained by pyrolysis. Joule heating was generated by an electric current circulating through this layer and the glass pane thus becomes a heating element. The total resistance of this heating film was measured at approximately 136 Ω, and its nominal power was 400 W. It is a few micrometers thick and covers the entire surface of the glazing, which is 1265 mm high and 680 mm wide. The incoming fresh air flows through the window from the outer to the inner openings that are 12 mm high and 355 mm wide, located in the upper part of the window frame.

A low emissivity layer (LE, AGC Planibel G) is on face 3 of the glazing and its role is typically to reduce thermal loss to the outside by long-wave heat radiation. This low-e layer is particularly useful when the heating film is active due to the significant radiation emitted from face 5. A thermal emissivity value of 0.14 was obtained from measurements carried out according to the NF EN 12898 standard [18].

2.3. Instrumentation

The three main physical quantities related to the operation of the window are airflow rate, the power of the heating film and the temperature of both the incoming and outgoing air.

The flow rate through the window was controlled using a micro pressure gauge (Furness Controls, FCO 510). The window was initially characterized by measurements of air flow and pressure drop through the window using a specific experimental set-up described in Ref. [6]. From these preliminary measurements, the air flow rate (Q) through the window was plotted as a function of the pressure gap (ΔP) between the inner and outer faces, as shown in Fig. 4. Subsequently, using these results, the flow rate could be determined from the pressure gap measurement. As an example, a flow rate of 15 m^3/h used in the present study was obtained for a pressure gap of 5.44 Pa. The maximum air flow rate uncertainty was estimated to ± 1.4 m^3/h.

The electrical power of the heating film was adjusted using a rototransformer type voltage converter. The supplied voltage and current were measured using two table-top multimeters (Aim-TTi) with measurement uncertainties of ±0.5% and ±0.8%, respectively.

Three temperature sensors were positioned within the ventilated air layers of the airflow window as shown on Fig. 5. In order to maintain the outdoor temperature ($T_{\text{air-out}}$) at its setpoint value, a PT100 temperature sensor, with an uncertainty of ±0.24°C, was placed at the outer window opening. The temperature measurements were used as the feedback for control the cooling capacity of the chiller in order to obtain the required outdoor temperature. Two other temperature sensors were installed at the bottom baffle ($T_{\text{air-baffle}}$), between the air layers L_1 and L_2, and at the inner window opening ($T_{\text{air-blowed}}$).

The K type thermocouples used for temperature measurements within the window, as well as the climatic cell (walls, roof and floor surfaces of the climatic cell) and the air conditioning system were first calibrated according to the Cofrac guidelines [19] using a Fluke 7321 thermostatic oil bath and a high-precision platinum resistance thermometer (PT100) of uncertainty ± 0.018°C. The

Fig. 2. Photo of the heated airflow window (sectional view).

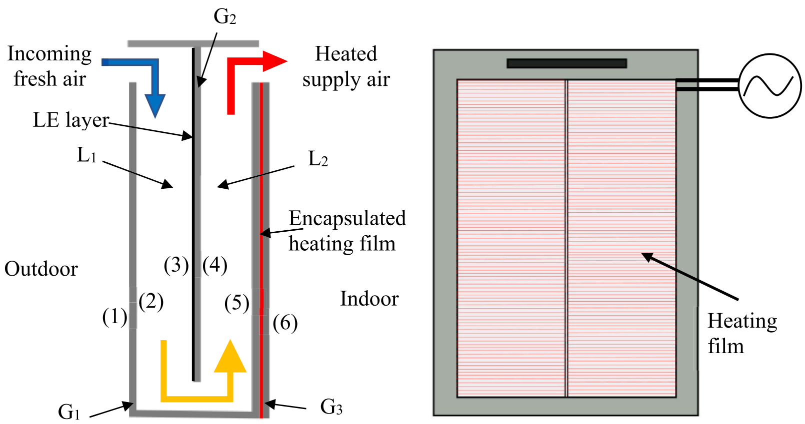

Fig. 3. Composition of the heating airflow window (left: side view; right: front view).

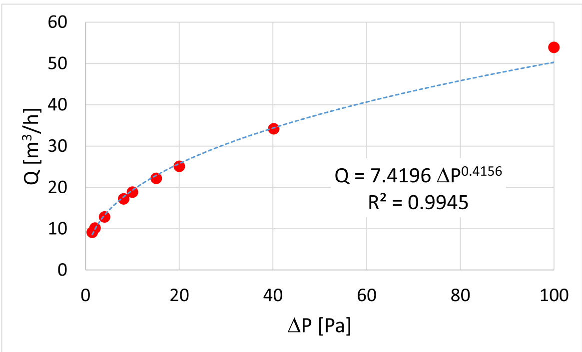

Fig. 4. Air flow rate through the window as a function of the pressure gap inside/outside.

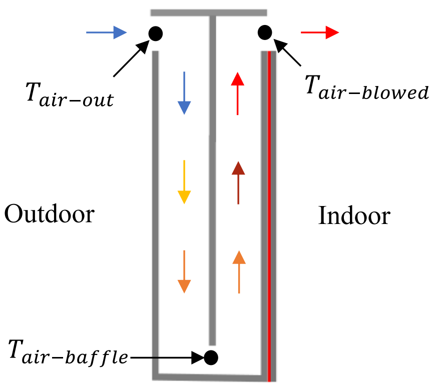

Fig. 5. Location of temperature sensors within the window.

thermocouple uncertainty was estimated to ±0.27°C using the methodology described in the Cofrac guide and the GUM [20]. Then, these thermocouples were connected to a Campbell Scientific CR1000 data acquisition unit equipped with 2 a.m.25T multiplexers. The acquisition frequency was set to 5 s.

The instrumentation of the climatic cell included wall and ambient air temperature sensors. A thermocouple was positioned on each wall of the climatic cell, while other thermocouples were added to measurement masts in order to assess the air temperature at several locations (detailed in the next section). Moreover, in order to measure the characteristics of the incoming air, a temperature and humidity sensor (type HMP45AC, Vaisala) was placed within the box simulating the outdoor environment (Fig. 1), that is just upstream of the air inlet of the window.

2.4. Methods and configurations

2.4.1. Method of assessing thermal comfort and air diffusion

The ASHRAE [21] defines the occupied zone as the interior volume located at a distance of 0.3 m from vertical walls and at a height of between 0.1 and 1.8 m from the floor. Fanger [22] suggested 3 height values for the determination of the thermal comfort indices: 0.2, 0.6 and 1.0 m from the floor for a seated person and 0.3, 1.0 and 1.7 m for a standing person. The ASHRAE Standard 55 [23] uses 0.1 (feet), 1.1 (center of gravity of the body) and 1.7 m (head) for a standing person. We used 4 heights to determine the thermal comfort indices, namely 0.1, 0.6, 1.2 and 1.8 m above the floor, as illustrated on Fig. 6. The heights of 0.1 m and 1.8 m are the limits of the occupation zone, 0.6 m corresponds to the center of gravity of a seated person. 1.2 m corresponds to the mid-point between 0.6 m and 1.8 m, in order to have a regular grid spacing, and it corresponds approximately to the center of gravity of a standing person and the head of a seated person.

The assessment of thermal comfort requires the measurement of four environmental parameters, namely air temperature, air velocity, ambient mean radiant temperature and relative humidity. Therefore, a set of sensors (see Fig. 6(a) and Table 1) was mounted on measurement masts in order to measure the first three parameters for the four vertical positions mentioned above (Fig. 6(b)). The last parameter, relative humidity, was maintained throughout the climatic cell using a dehumidifier located at the inlet of the fan coil which generated the airflow entering the climatic cell. The relative humidity value was continuously controlled during experiments using the temperature and humidity sensor located within the box simulating the outdoor environment, close to the air inlet of the window.

The sensors used are listed in Table 1, which also provides their main characteristics. All type K thermocouples were initially calibrated using a standard PT100 probe accurate to ±0.34°C, while the CO_2 sensors were calibrated using a standard CO_2 sensor (GMP 252).

Measurements were acquired using a measurement acquisition unit (Agilent Technologies, 34980A). The acquisition frequency for measurements related to the assessment of thermal comfort and air quality was set to 20 s.

The mean ambient radiant temperature was calculated from the overall temperature. For air velocity values less than 0.15 m/s, natural convection was dominant. Parsons [24] proposed the following correlation to evaluate the mean radiant temperature (T_{rm}) from the globe temperature (T_g) and the air temperature (T_{air}):

$$T_{rm} = \left[\left(T_g + 273\right)^4 + \frac{0.25\ 10^8}{\varepsilon_g} \left(\frac{\left|T_g - T_{air}\right|}{D} \right)^{0.25} \left(T_g - T_{air}\right) \right]^{0.25} - 273 \tag{1}$$

where ε_g is the surface emissivity of the black globe used ($\varepsilon_g = 0{,}97$) and D its diameter (D = 40 mm).

Finally, the air diffusion within the occupied zone was assessed using CO_2 as a tracer-gas. As shown by Fig. 6(c), this one was continuously injected into the air supply, just upstream of the box simulating the outdoor environment (Fig. 1). Note that according to this tracer-gas method, the CO_2 concentration represents here the fresh air diffusion rate, and not the occupant-generated CO_2 concentration, the climatic chamber being unoccupied.

As a consequence, a high CO_2 concentration at a given location downstream of the air outlet of the window indicates that this location is well ventilated. In other words and unlike normal indoor environments, a lower CO_2 concentration reflects here a poorer air renewal. Then, monitoring the CO_2 concentration within the occupied zone allowed an evaluation of the diffusion of fresh air coming from the window.

2.4.2. Configurations

Fig. 7 illustrates the four configurations that were used in the present study. The aim was to study the impact of a heated airflow window on comfort by comparison to more conventional windows. First, since the incoming air temperature is higher than the indoor

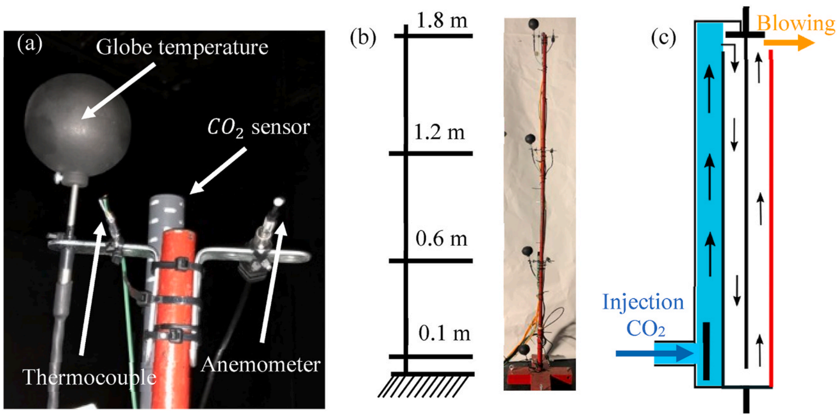

Fig. 6. (a) Measurement station, (b) Position of sensors along a measurement mast, (c) Injection of CO_2 used as tracer gas.

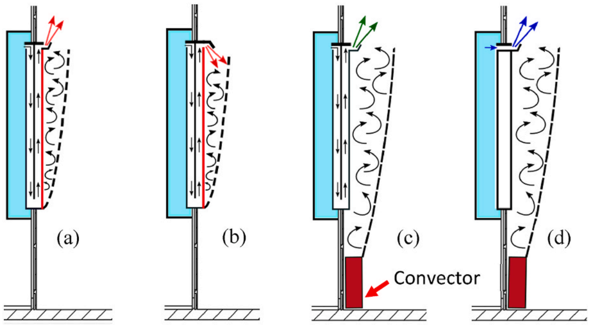

Fig. 7. Diagram of the tested configurations (a) HAW-up, (b) HAW-down, (c) AW-up-ec, (d) DGW-up-ec.

Table 1
Type and main characteristics of sensors used in the experimental set-up.

Sensors	Manufacturer	Type	Uncertainty
Relative humidity	Vaisala	Humicap®	±1% in the range 40 to 90% HR
Globe temperature	TC direct	Thermocouple K Globe: 40 mm	±0.34°C
Air temperature	TC direct	Thermocouple K	±0.34°C
CO_2 sensor	Vaisala	GMP 222 (0 to 3000 ppm)	±67 ppm
Omnidirectional anemometer	TSI	TSI 8475 (0.05 to 1 m/s)	±1% of selected measurement range

one in the case of a heated airflow window, air supplies pointing both upwards and downwards were tested, respectively designated by the “HAW-up” and “HAW-down” configurations in Fig. 7. The latter configuration was tested to evaluate whether reversing the orientation of the heated jet could improve the diffusion of the fresh air, and thus the air quality, by reducing the thermal stratification.

Then, an unheated airflow window was considered for the comparative study. The configuration called “AW-up-ec” on Fig. 7 combined this unheated airflow window and a conventional electric convector, located below the window. It must be specified here that, in practice, the window used for the HAW-up and HAW-down configurations as well as the AW-up-ec one was the same window described in Section 2.2. The difference between the HAW-up and HAW-down configurations was the orientation of the air outlet, while the heated glazing was active for the HAW-up and HAW-down configurations and inactive for the AW-up-ec one. Moreover, the window being identical for these three configurations, the same flow rate/pressure drop curve provided by Fig. 4 was used to maintain an airflow of 15 m^3/h for all these configurations.

Finally, a reference case was considered when conducting the comparative study. This one was defined as a combination of a conventional double-glazed window with the same electric convector used in the AW-up-ec configuration, located below the window. For this reference configuration, called “DGW-up-ec” on Fig. 7, the air inlet was directed upwards in order to reduce the cold draught effect. It can be noted here that for this more common configuration the fresh air entered the room directly through the air inlet

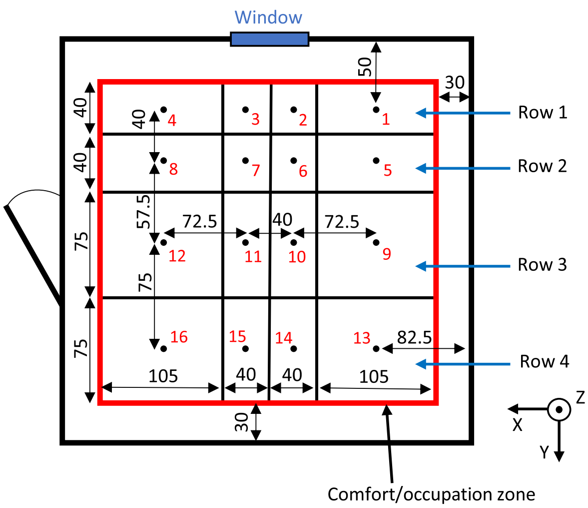

Fig. 8. Top view of the climatic cell showing the location of the measurement masts (centimeter scale).

(instead of through the glazing). As a consequence, in that case the flow rate was directly adjusted from the conventional air inlet characteristics and using the same micro pressure gauge than for airflow windows (see Section 2.3).

2.4.3. Experimental procedure and test conditions

The measurements were carried out in the entire volume of the occupied zone by dividing the latter into 64 sub-volumes in the center of which the environmental parameters were measured. As illustrated on Fig. 8 16 measurement masts were positioned along 4 rows (4 measurement masts per row) and each mast was equipped with 4 measurement stations (Fig. 6(b)).

For each sub-volume, the thermal comfort and discomfort indices were determined from measurements of temperature and velocity. Fig. 8 indicates that the mesh of the occupied zone was thinner close to the window than away from it. This type of meshing was adopted since the experimental parameters (outside temperature, incoming airflow rate and film power) had a more significant effect in the immediate vicinity of the window.

Temperature and velocity were measured in steady state conditions, the results were averaged over a 4-h period and are presented below in the form of tables using an identical color scheme for the 4 configurations. These tables show the geometry of the climatic cell. Four values are given within each volume, representing the 4 measurement heights, from top to bottom.

A comparative study of thermal comfort in the different configurations was carried out using the temperature and velocity measurements and the calculation of two comfort indicators (*PMV*, *PPD*). The sources of thermal discomfort were evaluated on the basis of the vertical temperature gradient and radiation asymmetry.

All tests were carried out for an outside air temperature of 5°C, representing winter conditions for cold climates, and a fresh air flowrate of 15 m^3/h, representing the air change rate of a small bedroom (air change per hour ACH = 0.4). The temperature setpoint for the active walls of the climatic cell was maintained at 19.5°C while the nominal power of both the heating film and the convector were set at 400 W. For each test, the acquisition time was about 4 h, both the stability and the uniformity of the environmental parameters measured were checked and their time-averaged values were calculated after at least 1 h of stabilization. The test duration for each configuration (HAW-up, HAW-down, AW-up-ec and DGW-up-ec) was 6 h in order to reach steady state conditions, and mean values were calculated from the last 10 min.

Note that in practice, when the heating was provided by the film, part of this heating was lost through the glazing of the window due to direct transmission to the outside environment. In contrast, when the heating was provided by the convector, thermal loss was lower since the heating element was not directly exposed to the outside environment. Consequently, the effective power delivered to the indoor environment was higher for the AW-up-ec and DGW-up-ec configurations than for the HAW-up and HAW-down configurations. Furthermore, since the airflow window (AW-up-ec) had a lower thermal loss in comparison to the conventional window (DGW-up-ec), as mentioned in Section 1, the power delivered to the indoor environment was greater for AW-up-ec than for DGW-up-ec. In this study, the tests were carried out with the same heating power, and therefore the same electricity consumption, and not with the same heat effectively provided to the indoor environment. This comparative was thus conducted from the user point of view, that is for an equivalent energy consumption for heating. However, results provided in the following section are presented and analyzed keeping in mind that the HAW configurations were penalized due to the direct thermal transmission through the glazing to the outside environment.

3. Results and discussion

3.1. Preliminary results

Table 2 provides the temperature values measured in several locations for each configuration considered. In this table, $T_{\text{glass-mean}}$ corresponds to the average temperature on face 6 of the window while $T_{\text{convector-mean}}$ corresponds to the average temperature on the surface of the convector. A preliminary determination of these two surface temperatures was obtained with infrared thermography [16].

Several observations can be made from these results.

- The air temperature at the baffle ($T_{\text{air-baffle}}$) was higher for the HAW configuration than for AW-up-ec due to the proximity of the heating film;
- The blowing temperature ($T_{\text{air-blowed}}$) could reach about 37°C for the HAW configurations, corresponding to a preheating air temperature of more than 30°C;
- The surface temperature of the glazing inner face, $T_{\text{glass-mean}}$, greatly varied from one configuration to another. For HAW, the surface temperature of the glazing was obviously higher than for DGW-up-ec since it is in direct contact with the heating film. In

Table 2
Temperature measurements for each tested configuration.

Temperature (°C)	HAW-up	HAW-down	AW-up-ec	DGW-up-ec
$T_{\text{air-baffle}}$	12.6	12.6	7.6	---
$T_{\text{air-blowed}}$	37.2	36.7	15.8	6.2
$T_{\text{glass-mean}}$	46.5	46.5	13.5	18.0
$T_{\text{convector-mean}}$	---	---	31.0	31.0

contrast, for the AW-up-ec configuration, the surface temperature of the glazing was lower than for DGW-up-ec since, in this case, the air flowing just behind the inner glass pane was cold.

3.2. *Thermal comfort*

3.2.1. *Measurements*

3.2.1.1. Air velocity. Fig. 9 provides, for the 4 configurations studied, the air velocity mean values (v_{air}) measured within the 64 sub-volumes previously defined. One can observe that the obtained values were particularly low, with a maximum of 0.1 m/s. Similar results were obtained by Myhren and Holmberg [25] for a dwelling heated with a medium temperature heating system. However, this was here a critical observation since, as specified in Table 1, the omnidirectional anemometers provided reliable results for an air velocity greater than 0.05 m/s according to the manufacturer. As a consequence, observations made from Fig. 9 were partly qualitative even though some trends can be deduced from these observations and from the comparison of one configuration to another. Thus, it can be observed on Fig. 9 that the distribution of the air velocity values in the occupied zone was relatively similar for both the HAW-up and HAW-down configurations. For these configurations, air movements were detected in the vicinity of the window, even if very

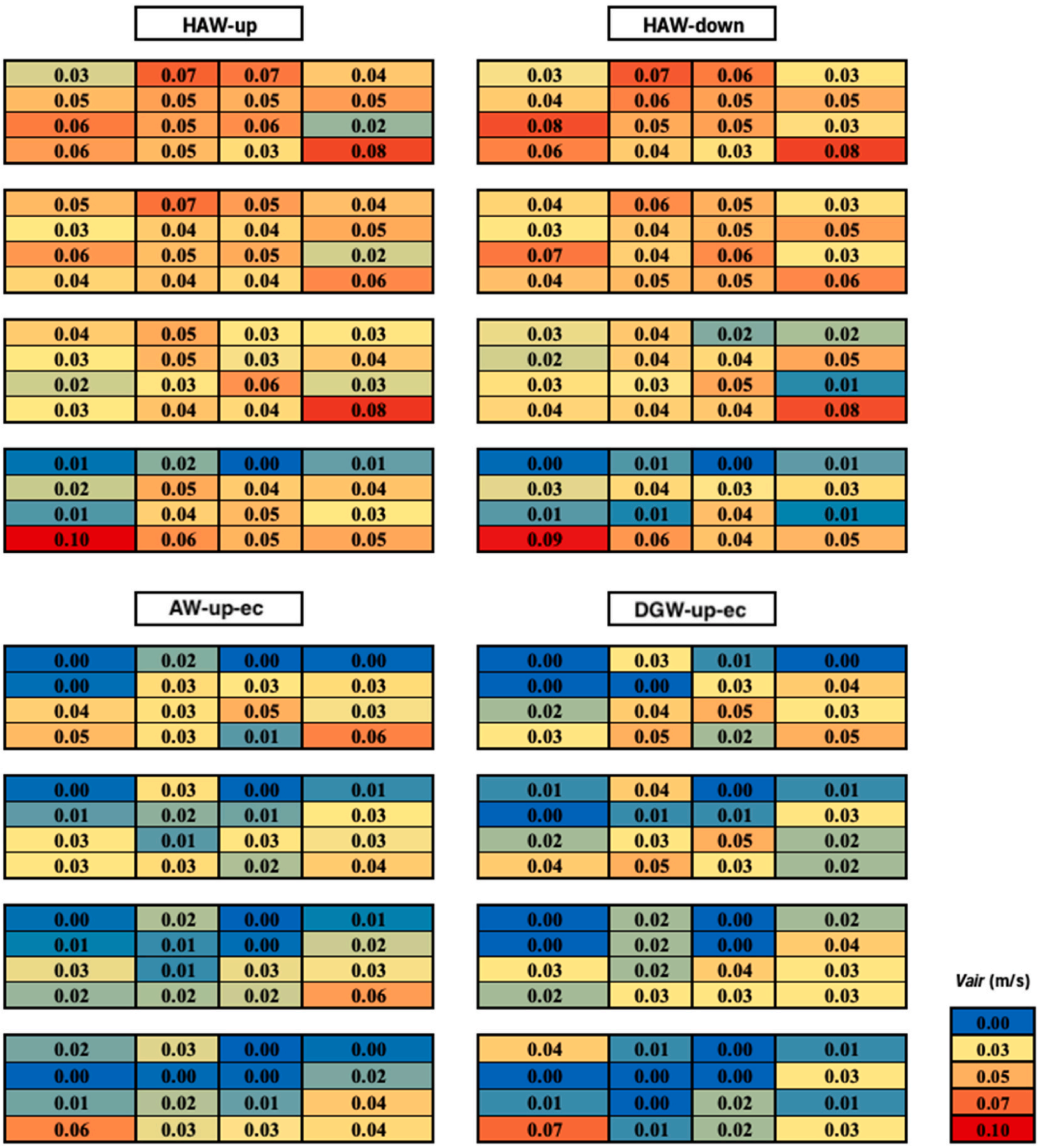

Fig. 9. Air velocity values measured at the 64 locations within the occupied zone.

weak, at the first 2 rows and more precisely at the measurement mast positions n° 2, 3, 6 and 7. This did not seem to be the case for the AW-up-ec and DGW-up-ec configurations. This difference between heated and non-heated windows could be explained, on the one hand, by the free convection flow induced by the heating film and, on the other hand, by jet-like flows from the air inlet grille. Indeed, for the HAW-up and HAW-down configurations, the incoming air was blown at approximately 37°C (see Table 2). It was therefore less dense than the air in the room and thus rose directly above the occupied zone (regardless of the orientation of the supply jet) and adhered to the ceiling. At the same time, when the free convection flow induced by the heating film reached the top of the window, it seems to be blocked by both the window frame and the jet-like flow from the air inlet grille. Such a blocking effect could induce a disturbance in the occupied zone and be responsible for the weak air movement detected in front of the window.

For the AW-up-ec and DGW-up-ec configurations, the temperature of the air was lower than that of the air in the room (see Table 2) and therefore this incoming air tended to flow downward within the occupied zone. However, the results suggests that it was then lifted by the plume induced by the electric convector of higher momentum. As a result of this interaction between the jet-like flow from the air inlet grille and the plume that developed above the convector, the incoming fresh air seems to move upward, towards the ceiling. This may explain that the air disturbance occurred above the occupied zone and not in front of the window.

The similarity of the velocity results obtained with heated windows for the HAW-up and HAW-down configurations led to the conclusion that changing the inlet from an upward to a downward direction did not significantly affect the airflow within the occupied

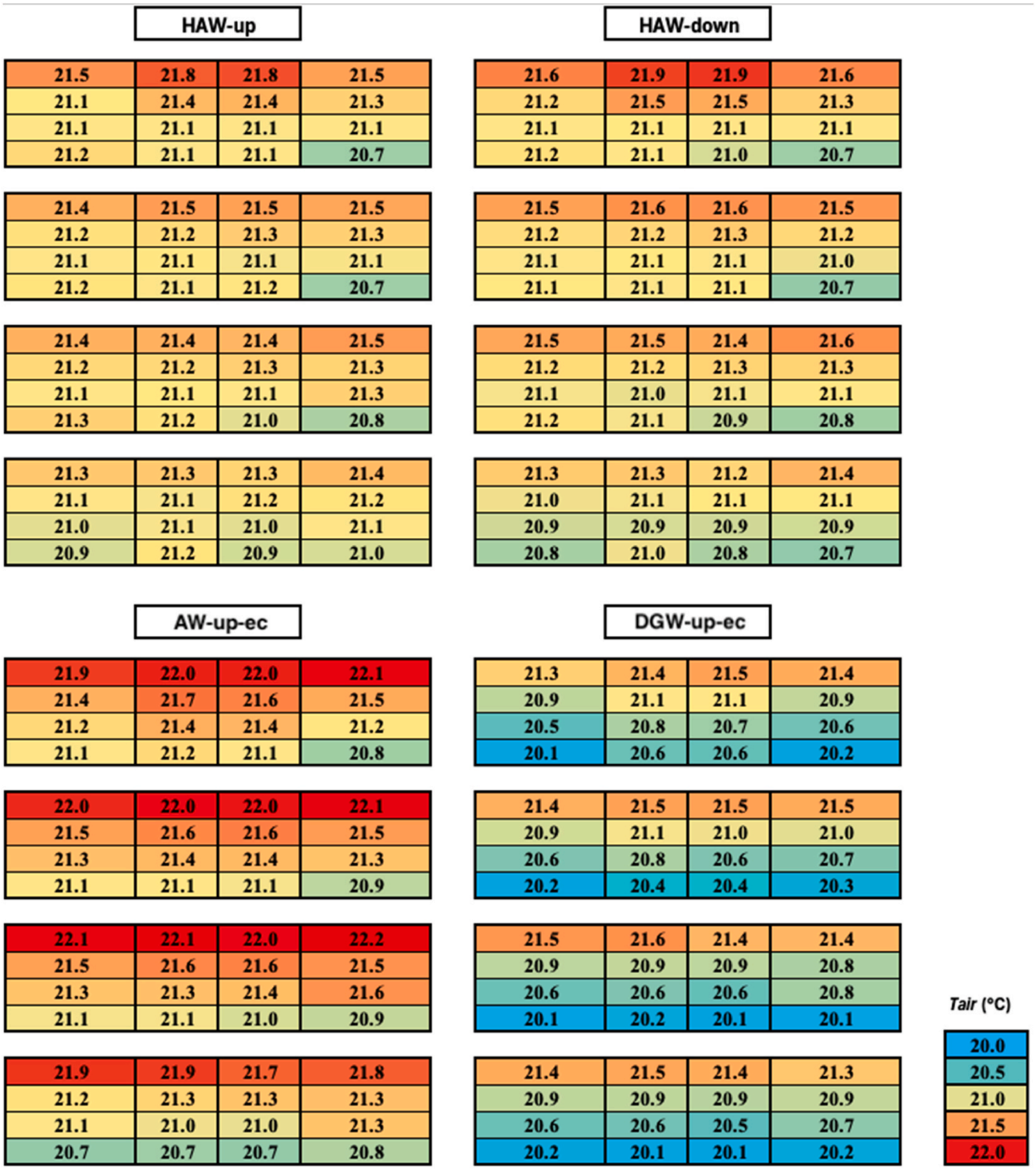

Fig. 10. Air temperature values measured at the 64 locations within the occupied zone.

zone. For other configurations, with non-heated windows, since results suggest that the plume rising from the convector was the dominant flow, the incoming fresh air flowed under the ceiling, above the occupied zone, and so air movements within this zone remained weak.

3.2.1.2. Air temperature. Fig. 10 provides the results obtained for air temperature (T_{air}). As previously observed with velocity, the air temperature results for the HAW-up and HAW-down configurations were relatively similar. The temperature significantly varied from one row to another. This is due to the air movement around the heated airflow window that improves air mixing and consequently temperature homogenization within the occupied zone. As expected, the air temperature was higher near the top window (heights of 1.2 and 1.8 m on measurement masts n°2 and 3).

For the AW-up-ec configuration, the temperature values measured in the occupied zone were the highest because the incoming fresh air was preheated when flowing through the glazing. The power supplied by the electric convector was added to this air preheating of about 16°C (see Table 2). As a result, for this configuration, the total heat provided to the occupied zone was greater than 400 W and, therefore, to the one transferred to the indoor environment by the heated glazing. Indeed, it must be remembered here that, for an identical power consumption, the effective power delivered by the HAW to the indoor environment was lower, due to higher direct thermal transmissions through the glazing to the outdoor one. It can also be observed on Fig. 10, for the AW-up-ec configuration, that the temperature distribution was similar in the first three rows, while the temperature was about 0.3°C lower in the fourth row. This indicates that the temperature distribution was not homogeneous throughout the occupied zone. Furthermore, the temperature levels in the upper part of the occupied zone were higher than those in the lower part, indicating the existence of thermal stratification in the occupied zone.

Conversely, for the DGW-up-ec configuration, the temperature measured in the occupied zone was the lowest. This was due to the low temperature of the incoming fresh air, which was close to 6°C (see Table 2), and the heat loss through the conventional double-glazing that was higher in comparison to a non-heated airflow window. For the DGW-up-ec configuration, the temperature distribution was quite similar from one row to another, and thermal stratification was more pronounced in comparison to the AW-up-ec configuration.

Fig. 11 presents the vertical temperature profiles obtained for rows 1 to 4 for the four configurations. The temperature profiles obtained for the HAW-up and HAW-down configurations are quite similar whatever the row, with a vertical temperature gradient of about 0.7°C in the first row and 0.5°C in the other rows. Such low differences in temperature reflect a homogeneity of temperature in the occupied zone.

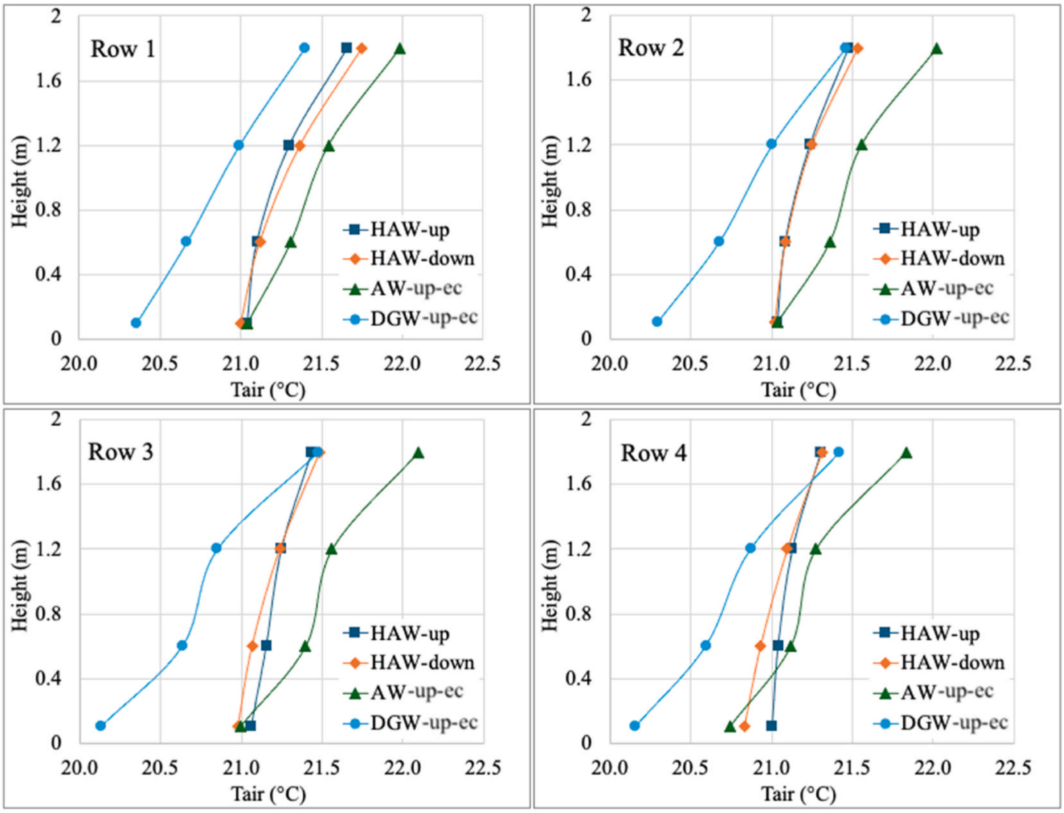

Fig. 11. Vertical profiles of the air temperature for the four rows and all tested configurations.

For the AW-up-ec configuration, the vertical temperature gradient was higher and almost constant for all rows, with a value close to 1°C. For the DGW-up-ec configuration, the vertical temperature gradient was higher too, increasing from 1°C for the first row to 1.4°C for the following rows.

Generally speaking, thermal stratification was more pronounced for the AW-up-ec and DGW-up-ec configurations than for HAW. For the latter configurations, the air movement in the occupied zone previously identified led to a mixing of the air and, subsequently, to temperature homogenization in this zone. In contrast, for the AW-up-ec and DGW-up-ec configurations, the absence of significant air movement led to a stronger thermal stratification in the occupied zone.

3.2.1.3. Mean radiant temperature. Fig. 12 provides the results of radiant temperature (T_{rm}) calculated from Eq. (1) and for which the maximum uncertainty was estimated to ± 0.8°C. The results obtained for the HAW-up and HAW-down configurations were quite similar. The radiant temperature was higher in the immediate vicinity of the heated airflow window, especially in the upper part (heights of 1.2 and 1.8 m on measurement masts n°2, 3, 6, 7), since the radiative exchange with the heated film was high locally. As the distance from the window increased the T_{rm} decreased and became relatively homogeneous at rows 3 and 4.

For the AW-up-ec and DGW-up-ec configurations, the values were lower and the radiant temperature distribution was relatively

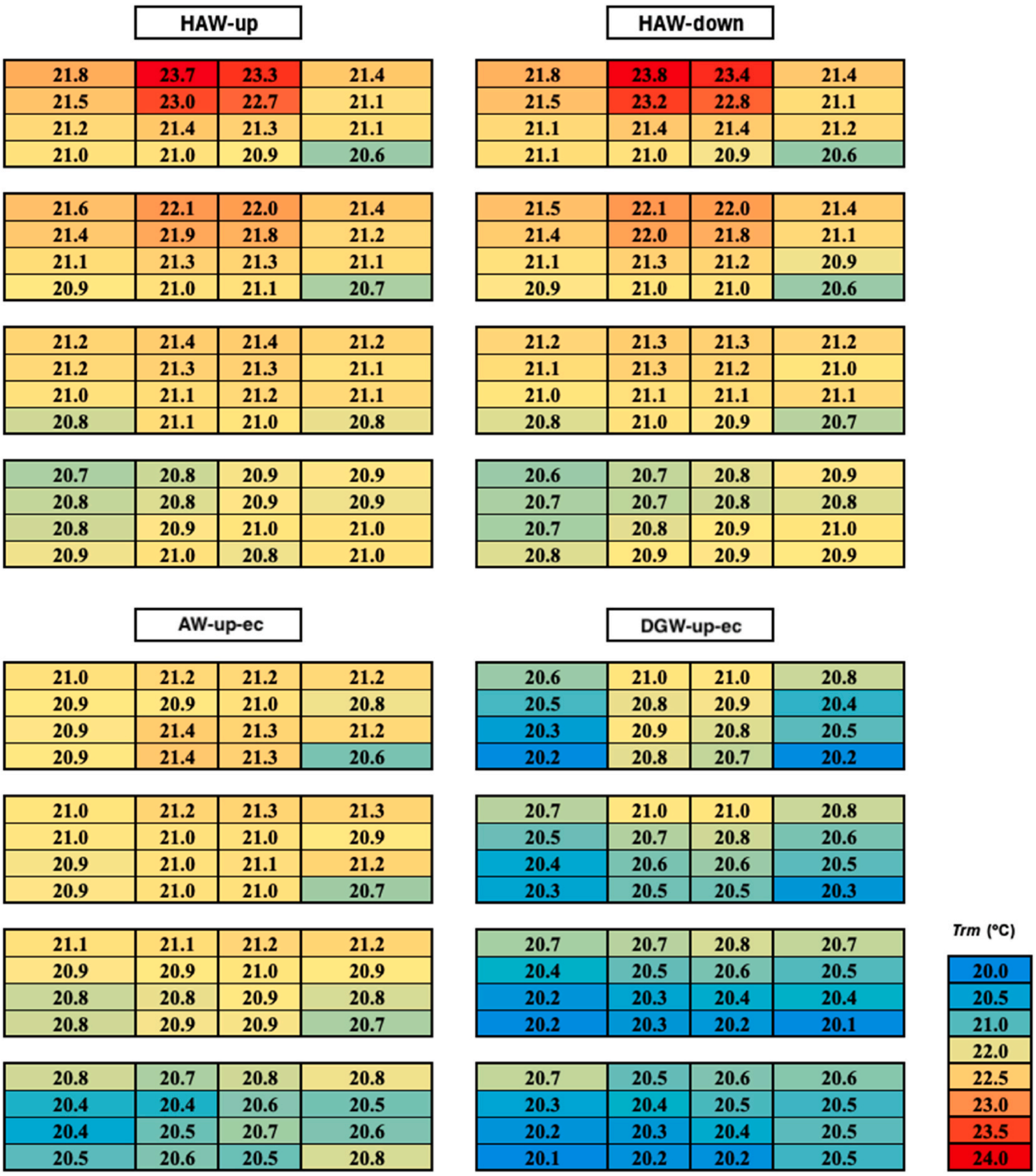

Fig. 12. Mean radiant temperature values calculated at the 64 locations within the occupied zone.

homogeneous at rows 1, 2 and 3. However, as expected, the radiant temperature values were high near the convector, and lower at row 4, which is located far from the convector.

In conclusion, the use of a heated airflow window increased the radiant temperature throughout the occupied zone, particularly in front of the window. The convector, which had a lower main surface temperature in comparison to the inner surface of the window, had therefore less effect than the heated glazing even if, as previously remembered, the effective power delivered by the HAW to the indoor environment was lower.

3.2.2. Thermal comfort indices

The calculation method provided by ANSI/ASHRAE Standard 55 [23] and ISO 7730 [26] was used to evaluate the *PMV* and *PPD* thermal comfort indices in the present study. The physical parameters used for these calculations are specified in Table 3. As indicated in Section 2.4.3, the climatic cell used was representative of a small housing room, typically a bedroom, in which a light activity was considered (sitting at desk, writing, reading, studying or standing), corresponding to a metabolic equivalent of task of 1.2 met [22,27] and a clothing level of 1 clo (typically a jacket and long pants).

The measured values for T_{air}, T_{rm} and v_{air} correspond to those provided in the previous section, measured at the 64 locations within the occupied zone, while, as specified in Sections 2.3 and 2.4.1, RH was measured using an humidity sensor located within the box simulating the outdoor environment, that is just upstream of the air inlet of the windows. This one was maintained at RH = 50 ± 1% using a dehumidifier located upstream of the incoming airflow.

Note that the PMV-PPD model was at first adopted here in order to assess the overall thermal comfort even though this commonly used model was initially built for stable and uniform indoor environments. However, mainly due to radiative effects of the window surface (cold surface for AW-up-ec and DGW-up-ec configurations, hot surface for HAW-up and HAW-down configurations) and of the electric convector one (used in configurations AW-up-ec and DGW-up-ec), the environment was actually non-uniform. Therefore, due to some local discomfort factors, PMV is not fully suitable for such a non-uniform radiant environment [28], and thus additional local thermal discomfort indices, introduced at the next section, were also assessed. The predicted mean vote, the *PMV* index, was determined from the heat balance of a human being and their environment, expressed as the following empirical law:

$$PMV = \left(0.303\, e^{(-0.036\, M)} + 0.028\right)\left(q_m - q_j\right) \tag{2}$$

where M is the metabolic rate, q_m the body heat production and where q_j represents human heat loss by radiation, convection, respiration and evaporation. Then, the predicted percentage of dissatisfied people, the *PPD* index, is related to *PMV* as follows:

$$PPD = 100 - 95\, e^{\left(-0.03353\ \mathrm{PMV}^4 + 0.2179\ \mathrm{PMV}^2\right)} \tag{3}$$

The *PMV* and *PPD* comfort indices were determined in the 64 sub-volumes of the occupied zone. The *PMV* and *PPD* index surface on Fig. 13and Fig. 14 were plotted by linear interpolation from the values calculated at the center of these sub-volumes.

3.2.2.1. PMV comfort index.

First of all, it can be noted that since the velocity values were low (Fig. 9), the *PMV* index mainly depends on T_{rm} and T_{air}. Fig. 13 shows the distribution of *PMV* for the four rows and for the four configurations studied.

As previously observed with velocity and temperature, quite similar results were obtained for the HAW-up and HAW-down configurations. The *PMV* index was higher in the vicinity of the window, meaning a more pronounced heat sensation due to both higher air and radiant temperature. In the remainder of the occupied zone, *PMV* distribution was generally homogeneous.

For the AW-up-ec and DGW-up-ec configurations, and in contrast to HAW-up and HAW-down, *PMV* was weaker in the lower part of the occupied zone and increased with height due to thermal stratification. The coldest thermal sensation was obtained for the DGW-up-ec configuration due to the low values of both T_{rm} and T_{air} (Fig. 10and Fig. 12).

For similar climate conditions and heating supply, it thus appears that the use of an airflow window led to a better heating of the occupied zone as well as a thermal comfort improvement for the occupants.

Table 4 provides statistical results for the *PMV* index. For each configuration, it gives the percentage of measurement points belonging to each thermal comfort category, as defined by ISO 7730 [26].

Table 4 shows that for the HAW-up, HAW-down and AW-up-ec configurations, more than 90% of the measurement points were in category A, and less than 10% of these points were in category B. The comparison between the HAW and AW-up-ec configurations pointed out that, even if the effective power delivered by the HAW to the indoor environment was lower, the thermal comfort was equivalent. For the DGW-up-ec configuration, only 61% of the measurement points were in category A, and 39% in category B. All four configurations can therefore be qualified as thermally comfortable since all of the measurement points were in categories A and B. However, the thermal comfort appeared to be slightly lower for the DGW-up-ec configuration in comparison to the three other configurations.

Table 3
Physical parameters considered (or measured) for PMV calculations.

Parameters	T_{air}	T_{rm}	v_{air}	*RH*	Metabolism [22,27]	Clothing [22,27]
Values	*measured*	*measured*	*measured*	50%	1.2 met = 70 W/m^2 (light activity)	1 clo (winter)

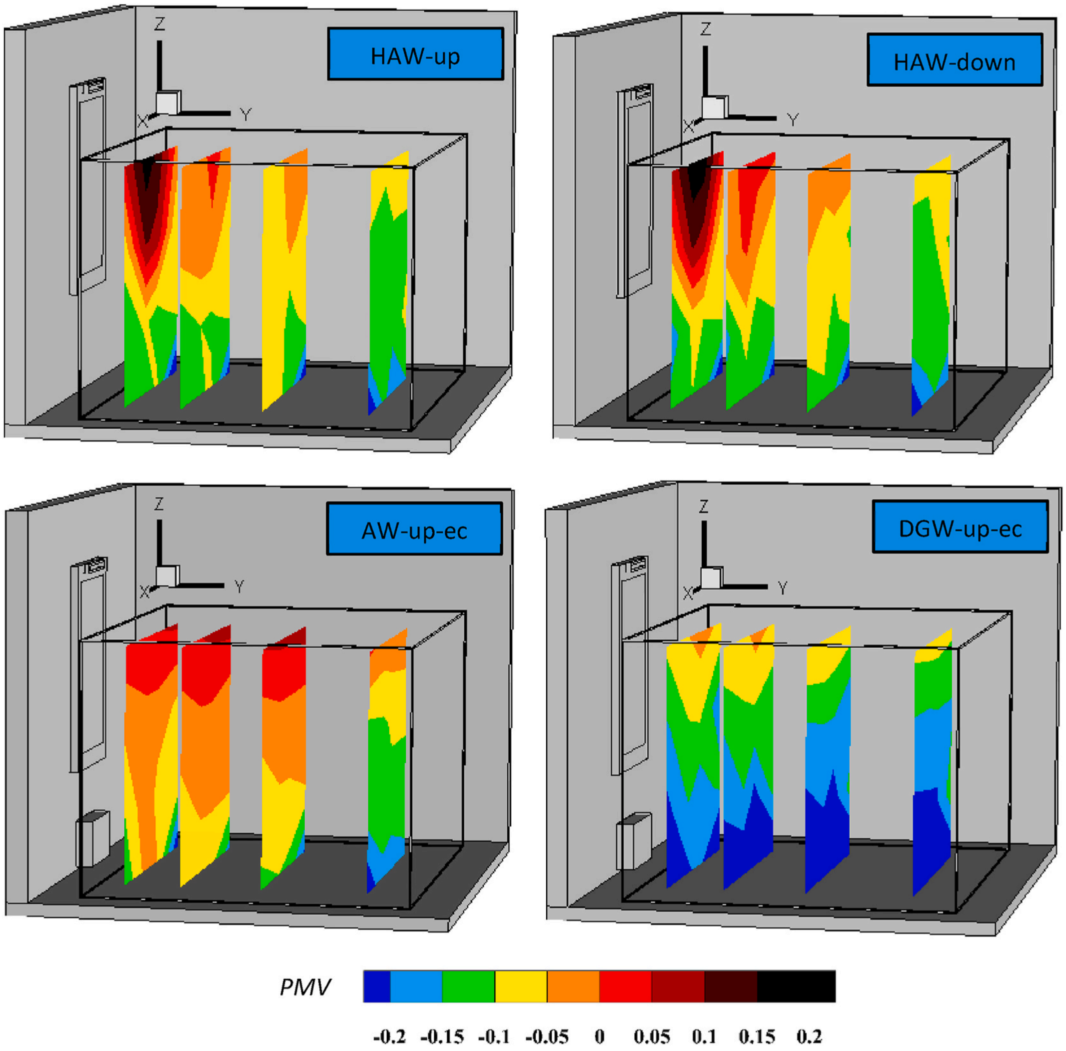

Fig. 13. Distribution of the PMV index within the occupied zone.

3.2.2.2. PPD comfort index. Fig. 14 shows the distribution of the *PPD* index for the four rows and the four configurations studied. For the HAW-up, HAW-down and AW-up-ec configurations, *PPD* distribution was homogeneous throughout the occupied zone. In contrast, for the DGW-up-ec configuration, the *PPD* values obtained in the lower part of the occupied zone were higher than in the upper part. The resulting feeling of coldness in the lower part of the occupied zone was due to a vertical temperature gradient.

Table 5 provides statistical results for the *PPD* index. Here again, for each configuration, it gives the percentage of measurement points in each thermal comfort category, as defined by ISO 7730 [26].

Table 5 shows that the highest number of measurements points in category A was obtained for the AW-up-ec configuration (97%). For the HAW-up and HAW-down configurations, the distribution of measurement points was the same: 94% in category A and 6% in category B. Finally, for the DGW-up-ec configuration, only 67% of the measured points were in category A. Here again, all four configurations can therefore be qualified as thermally comfortable since all the measurement points were in categories A and B. However, the thermal comfort appears to be slightly better for the AW-up-ec configuration in comparison to the HAW-up and HAW-down configurations, while it seems to be lower for the DGW-up-ec configuration.

All these observations led to the following main conclusions.

- For identical climate conditions and heating input, the heated airflow window provided better thermal comfort than a conventional double-glazed window associated with a convector.
- The orientation of the fresh air jet exiting a heated airflow window had no effect on the temperature and air velocity in the occupied zone and, consequently, on thermal comfort.
- Of the four configurations tested, the airflow window associated with a convector (AW-up-ec configuration) provided the best results in terms of thermal comfort.

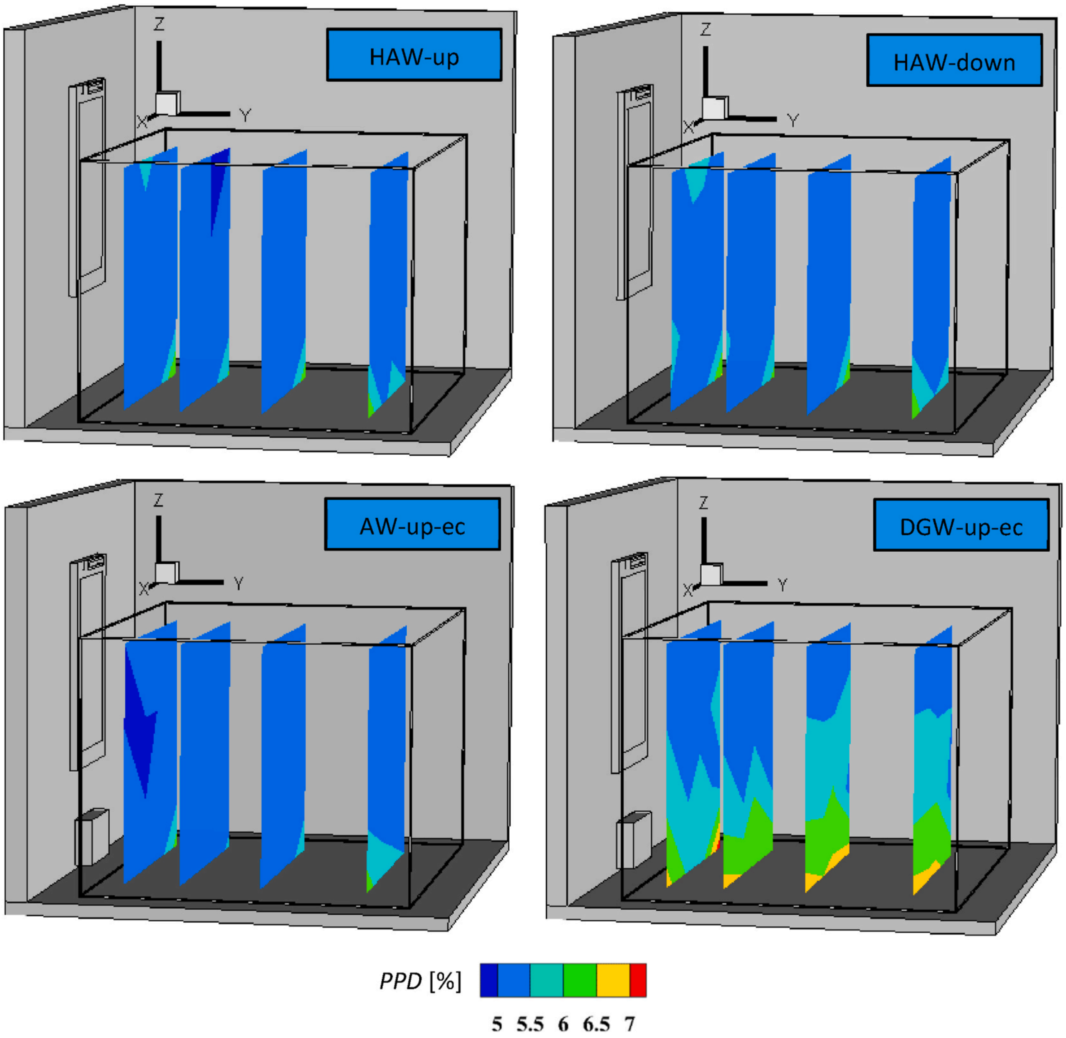

Fig. 14. Distribution of the PPD index (%) within the occupied zone.

Table 4
Percentage of measurement points belonging to each thermal comfort category for all tested configurations.

Category (ISO 7730)	Conditions	HAW-up	HAW-down	AW-up-ec	DGW-up-ec
A	$0.0 < \lvert PMV \rvert < 0.2$	94	94	95	61
B	$0.2 < \lvert PMV \rvert < 0.5$	6	6	5	39
C	$0.5 < \lvert PMV \rvert < 0.7$	0	0	0	0

Table 5
Percentage of measurement points in each thermal comfort category for all tested configurations.

Category (ISO 7730)	Conditions	HAW-up	HAW-down	AW-up-ec	DGW-up-ec
A	$0\% < PPD < 6\%$	94	94	97	67
B	$6\% < PPD < 10\%$	6	6	3	33
C	$10\% < PPD < 15\%$	0	0	0	0

- The difference in terms of comfort was significant if compared to the DGW-up-ec configuration (34% more measurement points in category A for the PMV index and 30% for the PPD index), but weak if compared to the HAW-up and HAW-down configurations (only 1% and 4% more measurement points in category A for the PMV and PPD indices, respectively).

The comparison between heated and unheated airflow windows pointed out here that the thermal comfort was roughly equivalent while, as previously specified, the effective heat supply to the indoor environment was higher for the AW-up-ec configurations in comparison to both the HAW-up and HAW-down ones. Due to the basis for comparison (same heating power for the convector and the heated glazing) and direct thermal transmission through the HAW glazing to the outside environment, more heat was transferred to the occupied zone using the AW-up-ec configuration (preheating of the entering air added to the heat provided by the convector). However, and even if the HAW configurations (up and down) were thus penalized in comparison to the AW-up-ec one, results pointed out that the thermal comfort was almost as high for an equivalent energy consumption for heating with a heated glazing and an electric convector, respectively.

3.2.3. *Local thermal discomfort indices*

The *PMV* and *PPD* indices provide indications on general levels of discomfort for the occupants. However, as specified in the previous section, this overall assessment is better suited in the case of a stable and uniform indoor environment. For a non-uniform radiant environment, here due to the window (as well as the convector when used), discomfort can be very local and four phenomena can induce local discomfort [26], namely.

- radiation asymmetry from the surfaces of the room (windows, walls, radiators, ceiling, etc.). It has previously been observed that the average radiant temperature is higher near heating elements (a heated window or convector) and varies from one configuration to another, while the temperature of the walls of the climatic cell was maintained at 19.5°C. Such differences in radiant temperature and walls temperature may be responsible for radiation asymmetry.
- the vertical temperature difference between the head and ankles of an occupant. The results obtained in terms of air temperature distribution within the occupied zone revealed a vertical temperature difference that varied depending on the configuration. Since the vertical temperature gradient remained weak, the resulting percentage of dissatisfied people was not significant either, but taking this index into account could provide an additional indicator of local discomfort.
- the draught risk and a floor that is too hot or too cold. In this study, the air velocity measured in the occupied zone was very weak while the floor temperature was maintained at 21°C for all configurations. Therefore, these parameters did not cause local discomfort in terms of draught risk and high or low floor temperature. Thus, they have not been taken into account here.

3.2.3.1. *Radiation asymmetry.*

The sources of radiation asymmetry [27] are the hot inner face of the window for the HAW-up and HAW-down configurations, and both the cold inner face of the window and the convector surface for the AW-up-ec and DGW-up-ec configurations.

The thermal discomfort caused by radiation asymmetry was characterized by the predicted percentage of dissatisfied people, which was determined by considering an occupant in front of the window and at different distances from it, namely 0.3, 1.45 and 2.6 m, as illustrated by Fig. 15.

According to ISO 7730 [26], the percentage of dissatisfied people (*PD*) due to asymmetry caused by a surface is given by:

$$PD_{ra} = \frac{100}{1+\exp\left(6.61-0.345\ |\Delta T_{pr}|\ \right)} \text{ for a cold surface} \tag{4}$$

$$PD_{ra} = \frac{100}{1+\exp\left(3.72-0.052\ \ |\Delta T_{pr}|\right)} - 3.5 \text{ for a hot surface} \tag{5}$$

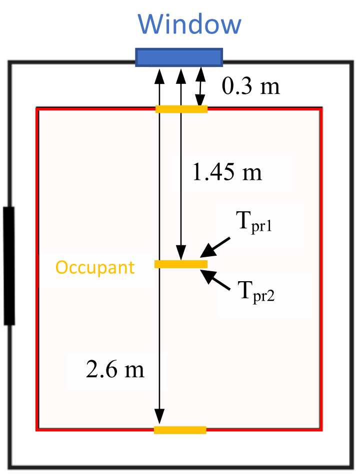

Fig. 15. Location of the occupant's silhouette, assumed to be rectangular, within the occupied zone (top view).

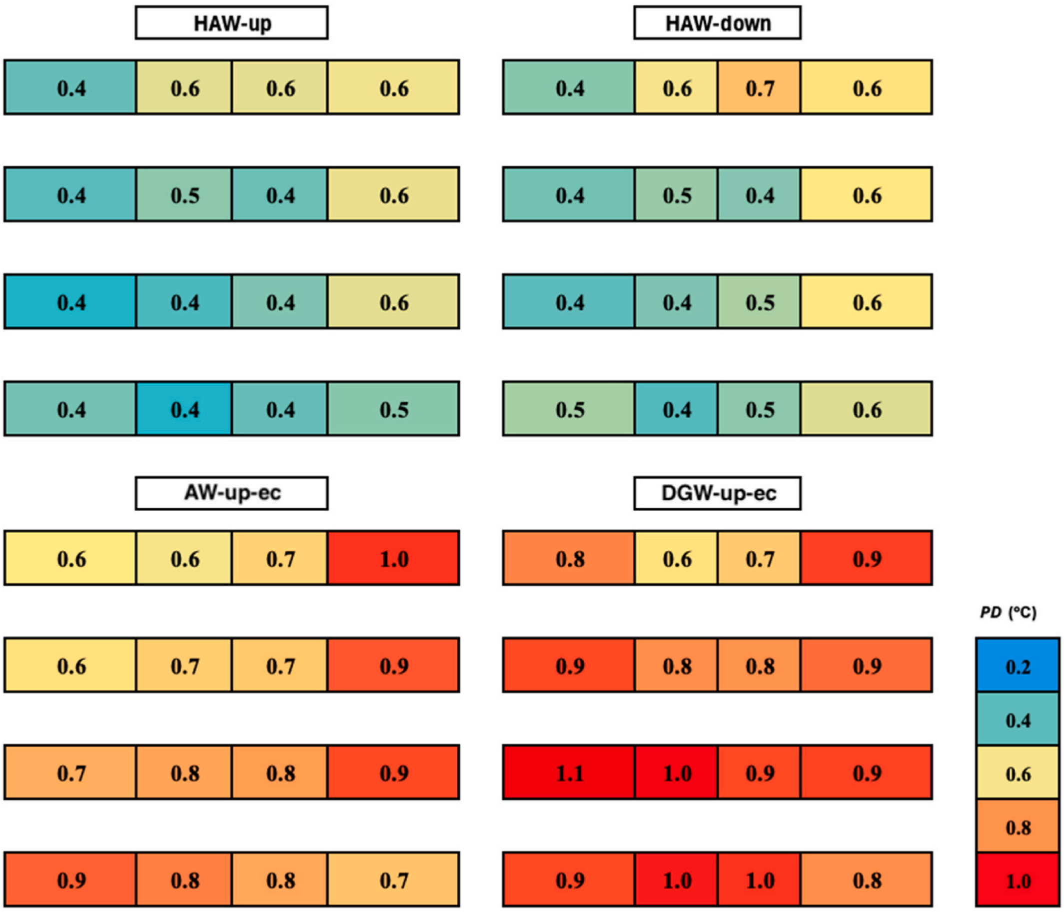

Fig. 16. Percentage of dissatisfied people due to a vertical temperature gradient obtained at the 16 measurement mast locations within the occupied zone.

where $\Delta T_{pr} = T_{pr1} - T_{pr2}$. ΔT_{pr} represents the radiant temperature difference between the two sides of the occupant's silhouette, which is assumed to be rectangular (its exposed and unexposed sides, as shown on Fig. 15).

$\Delta T_{pr} < 0$ means that the surfaces facing side 1 of the silhouette has a cold wall effect. In contrast, $\Delta T_{pr} > 0$ means that these surfaces have a hot wall effect.

The radiant temperature T_{pr} can be calculated from the temperature of the surrounding surfaces, and the view factors between the silhouette surface and the surrounding surfaces [29]. It is given by:

$$T_{pr} = \sqrt[4]{\sum F_{w-Aj}\, T_{Aj}{}^{4}} \tag{6}$$

where $F_{w\text{-}Aj}$ is the view factor for the radiative exchange between the rectangular surface of the silhouette and the opposite surface and T_{Aj} the temperature of the opposite surface.

Table 6 provides the radiant temperature difference and the PD_{ra} values obtained for all the configurations.

The results show that, for the heated airflow window, ΔT_{pr} was maximum (10°C) at a distance of 30 cm from the window. Nevertheless, the PD_{ra} value remained low (0.5%). Moving away from the window, ΔT_{pr} decreased and the PD_{ra} value fell to zero.

For the unheated airflow window, the ΔT_{pr} values were negative because the inner surface of the window was at a low temperature

Table 6
Radiant temperature difference, ΔT_{pr}, and percentage of dissatisfied people, PD_{ra}, for all the configurations tested.

	HAW-up, HAW-down (Eq. (5))		AW-up-ec (eq. (4))		DGW-up-ec (eq. (5))	
Distance (m)	ΔT_{pr} (K)	PD_{ra} (%)	ΔT_{pr} (K)	PD_{ra} (%)	ΔT_{pr} (K)	PD_{ra} (%)
0.30	10.0	0.50	−0.9	0.20	0.6	0.00
1.45	2.4	0.00	−0.3	0.15	0.1	0.00
2.60	1.0	0.00	−0.1	0.14	0.0	0.00

and the window surface is larger than that of the convector. In absolute value, ΔT_{pr} was also maximum at a distance of 30 cm from the window, which corresponds to a PD_{ra} value of 0.2%. This value decreased when the distance from the window increased.

It can be observed that, since the inner surface temperature of the double-glazed window (18°C) was very close to that of the walls (19.5°C), the temperature gap ΔT_{pr} was weak and did not suggest a significant risk of discomfort.

According to NF EN ISO 7730 [26], the thermal environment category A corresponds to a PD_{ra} index lower than 5%. Therefore, the 4 configurations studied here do not present a risk of thermal discomfort due to radiation asymmetry.

3.2.3.2. Vertical temperature gradient. Strong thermal stratification induces a large temperature difference between the ankles and the head. Even if the occupant is in a thermally neutral situation, this gap may be a source of thermal discomfort. In order to evaluate this, the percentage of dissatisfied people resulting from a vertical temperature gradient can be evaluated using the following empirical correlation [26]:

$$PD_{vtg} = \frac{100}{1 + \exp(5.76 - 0.856\ \Delta T_{a-h})} \tag{7}$$

where $\Delta T_{a\text{-}h}$ is the vertical air temperature difference between the occupant's ankles and head.

Fig. 16 shows the percentage of dissatisfied people for each measurement mast location.

According to standard 7730 [26], thermal environment category A corresponds to PD_{vtg} values lower than 3%. The PD_{vtg} values obtained were weak, with a maximum value of 1.1%. Therefore, none of the 4 configurations led to thermal discomfort caused by the vertical temperature gradient. However, Fig. 16 shows that PD_{vtg} values obtained for the HAW configurations were lower than for other configurations. This indicates that the risk of local thermal discomfort due to a vertical temperature gradient was reduced when a heated airflow window was used. These results are directly related to the air temperature measurements previously reported, and they indicate that thermal stratification was more pronounced for the AW-up-ec and DGW-up-ec configurations than for HAW.

In conclusion, the assessment of thermal comfort indices as well as of local thermal discomfort ones pointed out that all the four configurations can be qualified as thermally comfortable. However, the overall thermal comfort appeared to be slightly lower for the DGW-up-ec configuration, while it was observed that the risk of local thermal discomfort due to a vertical temperature gradient was reduced when a heated airflow window was used.

3.3. Air diffusion and IAQ

The results reported in the previous subsection have shown that, in comparison to the reference configuration DGW-up-ec and for an identical electrical power input, the use of an airflow window, whether for the configuration HAW-up, HAW-down or AW-up-ec, improved the thermal comfort. For these configurations involving the use of an airflow window, an additional study was conducted to investigate the air diffusion from the air inlet of the airflow window. The aim was to study the diffusion and distribution in the occupied zone of the fresh air blown by the airflow window in these configurations HAW-up, HAW-down and AW-up-ec.

As indicated in Section 2.4.1, CO_2 was here used as a tracer-gas. It was injected into the air supply just upstream of the box simulating the outdoor environment (see Figs. 1 and 6(c)) and, therefore, its concentration represented the fresh air diffusion rate. As a consequence, and unlike more usual situations for which a high CO_2 concentration, due to occupants, reflects a poor air renewal, a high CO_2 concentration at a given location downstream of the air outlet of the window suggested here a satisfactory local air renewal.

For each configuration tested, the CO_2 concentration was continuously measured at the 64 measurement station locations within the occupied zone (Figs. 6(a) and 8). The acquisition time was about 6 h and, after a stabilization period, results were obtained from a 2-h average of values of the CO_2 concentration. The experiments having been carried out over several days, therefore with a variable natural ambient CO_2 concentration, the results were normalized by the average value calculated from the 64 measurement stations for each tested configuration and whose maximum uncertainty has been assessed at 0.08. However, it was verified that these mean values obtained for the HAW-up, HAW-down and AW-up-ec configurations were close to a concentration of 2000 ppm (1957, 2025 and 2032, respectively).

Fig. 17 shows that the CO_2 concentration in the occupied zone was homogeneous for both the HAW-up and HAW-down configurations, indicating that air renewal was homogeneous. This homogeneity can be explained by the previously mentioned air movements that occurred close to the window, induced by both the heating film and the air inlet.

For the AW-up-ec configuration, and in comparison to others, the CO_2 concentration was low in rows 1 and 2 and increased significantly in rows 3 and 4. This result highlights the fact that the area covered by rows 1 and 2 was poorly ventilated and that the air quality was worse. In contrast, the area covered by rows 3 and 4 was well ventilated and the air quality was thus better. Here again, this result can be explained by the previously mentioned air movements that occurred close to the window. Indeed, for this configuration, the plume induced by the convector lifted the incoming air above the occupied zone (above rows 1 and 2) and then, at a certain distance from the window, moved downward and entered the occupied zone (rows 3 and 4).

It can be concluded here that, similarly to the results obtained for thermal comfort, the orientation of the air supply from the airflow window had no effect on the IAQ. The air movement induced by the heating film of the airflow window led to a better mixing of the incoming fresh air and the existing indoor air. Thus, in comparison to a non-heating airflow window, the IAQ was improved when the airflow window was heated.

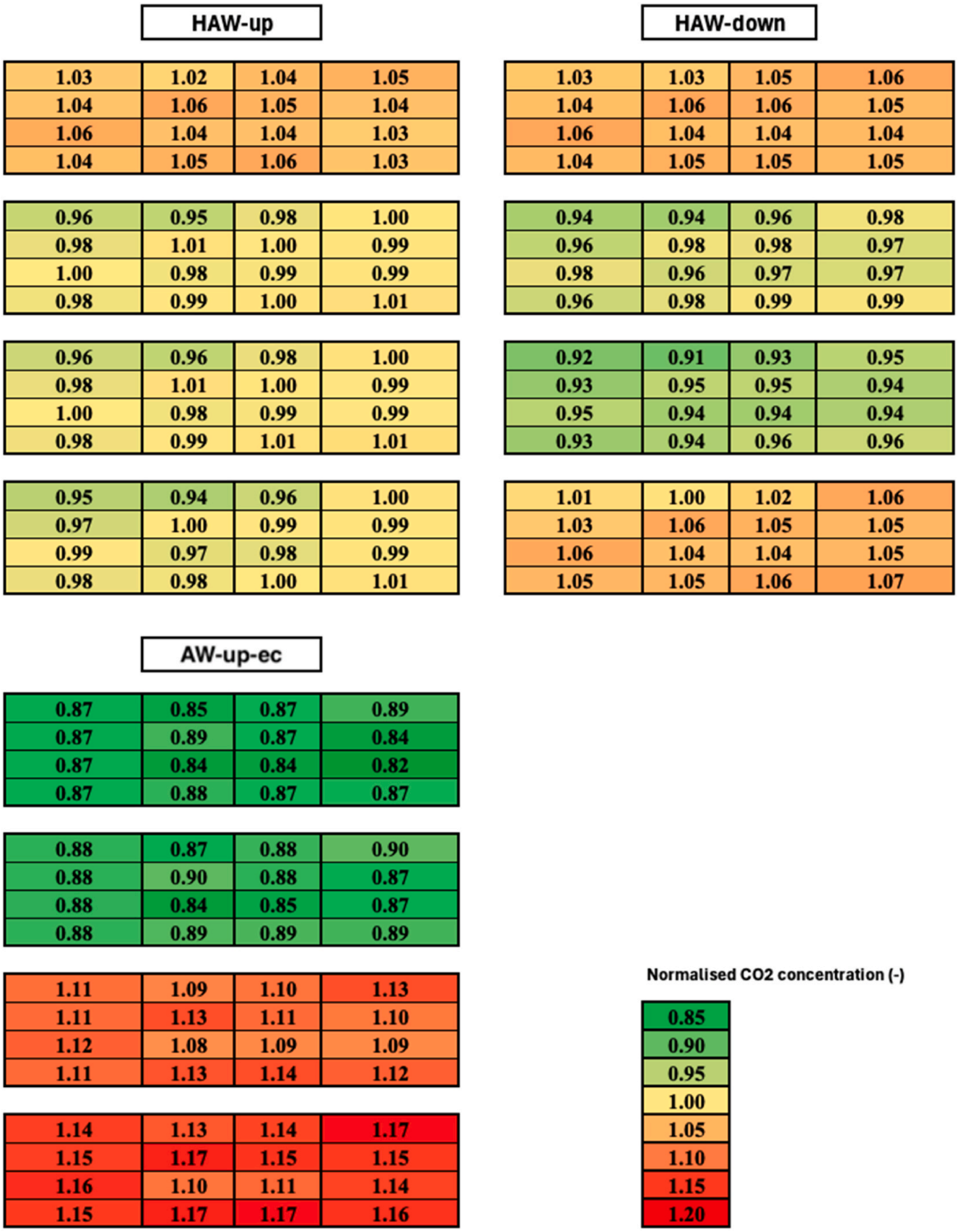

Fig. 17. CO_2 concentration normalized by the mean value calculated from the 64 measurement stations within the occupied zone.

4. Conclusions

In the context of building heating applications, the relevance of the combination of an airflow window and a heated glazing was investigated. Thus, an airflow window previously developed by the authors and composed of 3 glass panes with a single airflow has been improved by incorporating a heating film into the inner glass pane. The performance of the resulting heated airflow window was experimentally investigated in terms of thermal comfort and fresh air diffusion, and thus the IAQ. Four configurations were examined in this study, and then compared: two heated airflow windows with an upward or downward air discharge (HAW-up and HAW-down), an unheated airflow window combined with an electric convector (AW-up-ec), and a reference case corresponding to a conventional double-glazed window associated with the same electric convector (DGW-up-ec). This comparative study was conducted by considering the same heating power, *i.e.* the same electricity consumption of both the heating film (for the HAW-up and HAW-down configurations) and the convector (for the AW-up-ec and DGW-up-ec configurations).

The results show that the use of an airflow window, whether heated or not, improved the overall thermal comfort (more than 90% of the occupied zone in PMV category A) in comparison to the reference case (only 61% of the occupied zone in category A). However, the assessment of two local discomfort sources encountered in non-uniform radiant environment, radiation asymmetry and strong thermal stratification, pointed out that none of the 4 configurations led to a notable local thermal discomfort and that the risk of local thermal discomfort due to a vertical temperature gradient was slightly reduced when a heated airflow window was used.

The similarity between all the results obtained for heated and unheated airflow windows pointed out that, even if the effective power delivered by the first one to the indoor environment was lower in comparison to the second one, due to the direct thermal transmission through the glazing to the outside environment, the thermal comfort was equivalent for these two configurations.

In the case of a heated airflow window, it was observed that the reversal of the air discharge direction had no effect on thermal comfort. Indeed, for both configurations, the incoming fresh air rose above the occupied zone due to its high temperature. The heating film of the heated airflow window created a disturbance of the air in the occupied zone, which led to a better mixing of the indoor air. This in turn led to a reduction in thermal stratification in the occupied zone and in the percentage of dissatisfaction related to the vertical temperature gradient. For configurations with an electric convector, the thermal plume rising above the convector led to an increase in thermal stratification and thus in the percentage of dissatisfaction related to the vertical temperature gradient. It was also noted that the radiation asymmetry generated by the heated windows was not high enough to cause any local thermal discomfort.

Concerning the diffusion of fresh air, the study shows that the air movement induced by the heating film of the heated airflow window fostered a mixing between the incoming fresh air and the indoor air. Consequently, this led to a better fresh air diffusion, and thus a better IAQ, in comparison to the non-heated airflow window configuration. In this latter configuration, the lack of air movement in the occupied zone contributed to an inhomogeneous distribution of fresh air.

Although the reported comparative study was conducted for limited surrounding and operating conditions, the first experimental results obtained with the developed heated airflow window pointed out that the combination of an airflow window and a heated glazing could be relevant as expected for building heating applications. Mainly, by reducing direct thermal loss of the heated glazing to outdoor and "cold wall" effect observed for airflow windows. Furthermore, this comparative study in terms of thermal comfort and air diffusion was also limited by the basis for comparison (identical heating power for all tested configurations) that was, as specified in the paper, unfavorable for the heated airflow window. As a consequence, the present study should be expanded by additional scenarios (ambient conditions, airflow rate, heating power) as well as a specific study on the thermal efficiency of the heated airflow glazing, in particular to assess the effective heat provided by the heating film to the indoor environment.

CRediT authorship contribution statement

Alain Makhour: Investigation, Methodology, Writing – original draft. **Ghislain Michaux:** Conceptualization, Investigation, Methodology, Project administration, Resources, Supervision, Validation, Writing – original draft. **Patrick Salagnac:** Conceptualization, Funding acquisition, Investigation, Methodology, Project administration, Validation, Writing – original draft. **Pierre Bragança:** Methodology, Writing – original draft.

Declaration of competing interest

The authors declare that they have no known competing financial interests or personal relationships that could have appeared to influence the work reported in this paper.

Acknowledgments

The activities reported here were carried out within the framework of the "CPER Programme 2014-2020″ research project that was funded by the European Union and the French region of Nouvelle-Aquitaine. The authors would like to thank both of them for their financial support, as well as the Ridoret Company for providing the airflow window.

Data availability

Data will be made available on request.

References

[1] A. Shandilya, M. Hauer, W. Streicher, Optimization of thermal behavior and energy efficiency of a residential house using energy retrofitting in different climates, Civil Engineering and Architecture 8 (2020) 335–349, https://doi.org/10.13189/cea.2020.080318.
[2] W. Feist, J. Schnieders, Energy efficiency – a key to sustainable housing, Eur. Phys. J. Spec. Top. 176 (2009) 141–153.
[3] J. Tian, W. Cheng, M. Xiu, H. Zhang, C. Han, F. Ye, H. Tao, Y. Huang, Multifunctional smart windows: development and integration for smart net-zero buildings – a state-of-the-art review, Constr. Build. Mater. 495 (2025) 143524.
[4] J. Wei, J. Zhao, Q. Chen, Energy performance of a dual airflow window under different climates, Energy Build. 42 (1) (2010) 111–122.
[5] G. Michaux, R. Greffet, P. Salagnac, J.B. Ridoret, Modelling of an airflow window and numerical investigation of its thermal performances by comparison to conventional double and triple-glazed windows, Appl. Energy 242 (2019) 27–45, https://doi.org/10.1016/j.apenergy.2019.03.029.
[6] R. Greffet, Études Expérimentale Et Numérique Des Performances Énergétiques D'Une Fenêtre Pariétodynamique, La Rochelle, France, 2016. PhD.

[7] J. Kurnitski, J. Jokisalo, J. Palonen, K. Jokiranta, O. Seppänen, Efficiency of electrically heated windows, Energy Build. 36 (2004) 1003–1010.
[8] E.A. Ollokiegi, Electric Heated Windows: Thermal Comfort and Energy Use Aspects, University of Gävl, 2013.
[9] H.S. Jammulamadaka, Evaluation of energy efficiency performance of heated windows, in: Theory of Computing Systems, 2017, p. 4. *Mathematical Systems Theory*.
[10] R. Lee, E. Kang, H. Lee, J. Yoon, Heat flux and thermal characteristics of electrically heated windows: a case study, Sustainability (2022).
[11] H. Lee, K. Lee, E. Kang, D. Kim, M. Oh, J. Yoon, Evaluation of heated window system to enhance indoor thermal comfort and reduce heating demands based on simulation analysis in South Korea, Energies (2023).
[12] P.G. Krukovskyi, D. Smolchenko, G. Krukovskyi, A.I. Deineko, Analysis of the heating capacity of electrically heated windows, in: Thermophysics and Thermal Power Engineering, 2021.
[13] B. Basok, B. Davydenko, S. Goncharuk, A.M. Pavlenko, O. Lysenko, V. Novikov, Features of heat transfer through a window with electric heating, in: IEEE 8th International Conference on Energy Smart Systems (ESS), 2022, pp. 195–198.
[14] G. Ferla, C.A. Román, J.R. Calzada, Radiant glass façade technology: thermal and comfort performance based on experimental monitoring of outdoor test cells, Build. Environ. 182 (2020) 107075.
[15] C. Zhang, X. Xu, J. Yu, X. Tang, Z. Yu, Condensation risk-based applicability analysis and design of a dynamic thermal insulation window with ventilated airflow in different climates, J. Build. Eng. 86 (2024) 108913.
[16] A. Al Akbar Makhour, P. Bragança, G. Michaux, P. Salagnac, R. Greffet, Étude Des Champs De Température Obtenus Par Thermographie Infrarouge À La Surface Intérieure D'Une Fenêtre Pariétodynamique Chauffante, *XIVème CIFQ*, Québec, Canada, 2019.
[17] M. Kaboré, G. Michaux, J. Le Dréau, P. Salagnac, R. Greffet, Parametric study of the thermal performance of a single-family house equipped with an airflow window integrating a heated glazing, in: 16th International Conference of the International Building Performance Simulation Association, 2019, pp. 2020–2025. Rome, Italy.
[18] NF EN 12898, Glass in Building - Determination of the Emissivity, 2019.
[19] Cofrac, Guide technique d'accréditation en température, in LAB GTA 08, (n.d.).
[20] JCGM, GUM - Evaluation of Measurement Data — Guide to the Expression of Uncertainty in Measurement, 2008.
[21] ASHRAE - Handbook, Fundamentals (SI), 2009.
[22] P.O. Fanger, Thermal Comfort. Analysis and Applications in Environmental Engineering, McGraw Hill, New York, 1970.
[23] ASHRAE Standard 55–2013, Thermal Environmental Conditions for Human Occupancy.
[24] K. Parsons, Human Thermal Environments: the Effect of Hot, Moderate, and Cold Environments on Human Health, Comfort, and Performance, third ed., CRC Press, London, 2002, p. 635.
[25] J.A. Myhren, S. Holmberg, Flow patterns and thermal comfort in a room with panel, floor and wall heating, Energy Build. 40 (2008) 524–536.
[26] ISO 7730:2005, Ergonomics of the Thermal Environment — Analytical Determination and Interpretation of Thermal Comfort Using Calculation of the PMV and PPD Indices and Local Thermal Comfort Criteria.
[27] H.B. Awbi, Ventilation of Buildings, second ed., 2003. London.
[28] X. Su, Y. Yuan, Z. Wang, W. Liu, L. Lan, Z. Lian, Human thermal comfort in non-uniform thermal environments: a review, Energy and Built Environment 5 (6) (2024) 853–862.
[29] ISO 7726:1998: Ergonomics of the Thermal Environment — Instruments for Measuring Physical Quantities.